Available free online at www.medjchem.com

Mediterranean Journal of Chemistry **2015**, 4(2), 105-110

Corrosion Inhibition of AISI 316L and Modified-AISI 630 Stainless Steel by the New Organic Inhibitor $[(CH_3)_2N]_3PSe$ in Chloride Media:Electrochemical and Physical Study

Yafa Zargouni [1], Wafa Sassi [2,3] and Khaled Alouani [1,*]

[1] Laboratoire de chimie analytique et d'électrochimie, Faculté des Sciences de Tunis, Université de Tunis-El-Manar, 2092, Tunisie
[2] Laboratoire de Mécanique-Énergétique, ENIT, Université de Tunis-El-Manar, BP 37, Tunis Belvédère, 1002, Tunisie
[3] Institut UTINAM, CNRS UMR 6213, Université de Franche-Comté, 16 route de Gray 25030 Besançon Cedex, France

Abstract: The effect of Tris-dimethylaminoselenophosphoramide (SeAP) as corrosion inhibitor for modified-AISI 630 and AISI 316L stainless steel (SS) in 3 wt. % NaCl is investigated by potentiodynamic polarization, SEM and GDOES techniques. After adding SeAP at different concentrations) in 3 wt. % NaCl, Tafel slopes for both SS show that the efficiency of this inhibitor increases with its concentration. The morphological changes on stainless steel are checked before and after adding SeAP, at its optimal concentration, by scanning electron microscopy (SEM), and glow discharge optical emission spectroscopy (GDOES). Adsorbed on the surface, SeAP is found to be a good inhibitor for SS corrosion, especially when added at a concentration of 0.5 wt. %.

Keywords: Tris-dimethylaminoselenophosphoramide; corrosion inhibition; stainless steel; adsorption.

Introduction

Among the various corrosion prevention measures applied in numerous fields, the corrosion inhibitors have been known for their high-efficiency and their wide range of application. In this context, the use of organic inhibitors is one of the most practical and cost-effective methods to protect metals from corrosion [1], especially in chloride media.
The efficiency of this type of compounds is related to several factors such as: the charge distribution in the molecules, the presence of heteroatoms and the contained functional groups as P=Se, P–N [2-4]. These inhibitors are usually adsorbed chemically (covalent bond) or physically (electrostatic interaction) on the metal surface.

Phosphorous compounds were known as efficient corrosion inhibitors for a variety of materials in neutral and slightly alkaline aqueous solutions. In recent years, exhaustive practical experience has highlighted the importance of the phosphate in corrosion inhibition of iron and its alloys [5-6]. However, to our knowledge, there is no study on how phosphorus compounds affect stainless steel corrosion in the presence of chloride.

Among stainless steel types, AISI 316L is well known for its high corrosion resistance and it is frequently used in piping systems and wastewater treatment plants [7-8]. The AISI 630 (or 17-4PH) [9,10,11] is another type of stainless steel with a moderate corrosion resistance but famous for its excellent mechanical properties. AISI 630 is commonly used for manufacturing components and petroleum industry [12]. AISI 316L and AISI 630 are often susceptible to corrosion and severe damages in presence of chloride ions[13]. For the reasons mentioned above, the investigation of stainless steel corrosion behavior and the protection of such materials are of a practical importance.

The present work reports the efficiency of the Seleno-Tris (dimethyl-amino-phosphine) (SeAP)[14] as a new inhibitor of stainless steel corrosion in sodium chloride solution.

The choice of this compound to be tested as an inhibitor was based on molecular structure considerations. SeAP has three nitrogen atoms and

**Corresponding author: Khaled Alouani*
E-mail address: khaled.alouani@gmail.com
DOI: http://dx.doi.org/10.13171/mjc.4.2.2015.21.04.12.05/alouani

one phosphorus atom, which are assumed to be an active center of adsorption.

Experimental Section

Materials and optimization

The inhibitor was synthesized according to the following procedure reported in the literature[14]. The purity of the SeAP was confirmed by NMR^{1}H (Figure 1)

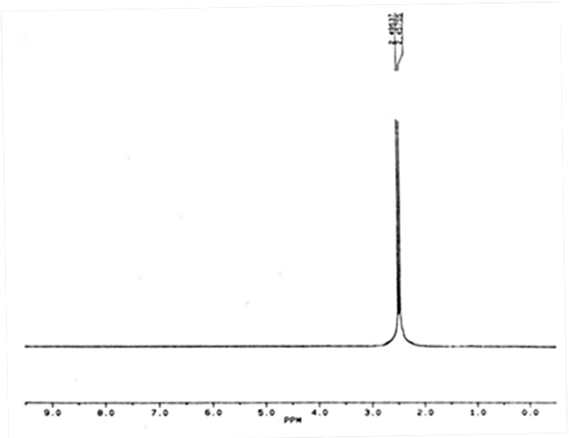

Figure 1. NMR ^{1}H (NMe_2) P=Se (Solvent: $CDCl_3$)

The electrode rotation speed and the content of the SeAP into the chloride media are very important to optimize a resistant adsorbed layer against chloride ions penetration and to improve the corrosion inhibition in the shortest time possible.

A Doehlert design, with $3^2 = 9$ experiment (3 levels and 2 factors), was carried out as a screening approach to optimize those experimental conditions using NEMROD software program (L. P. R. A. I, Marseille, France). The polarization resistance values Rp of SS samples immersed into 3 wt.% NaCl and into 3 wt.% NaCl + SeAP used as responses in Doehlert design were investigated and described elsewhere [15].

Fresh solutions of the 3 wt. % sodium chloride at pH of 7 were prepared for each experiment using analytical grade of pure NaCl and distilled water. The temperature was 20 ± 2°. The inhibitor concentration in the 3 wt. % NaCl corrosive media was achieved by adding aliquots of SeAP from a stock solution of 10 g dm^{-3}. The SeAP is not toxic within the range of concentration adopted. After adding the inhibitor to 3 wt. % NaCl solution, the measured pH of the mixture was 6.8.

Electrochemical potentiodynamic polarization

Electrochemical polarizations experiments were carried out in a three-electrode cell using a potentiostat–galvanostat Radiometer Copenhagen PGZ 402 model, piloted by Voltlab4 software. A saturated calomel electrode (SCE) was used as a reference electrode and a Pt electrode as a counter.

Working electrodes (the tested samples) were prepared from rectangular coupons (1 cm^2) of modified-AISI 630 and AISI 316L stainless steel. The modified-AISI 630 used in this study was the main material forming the piston in a water pump installation of the petroleum rig in Oudhna North of Tunisia. It was mentioned that the composition of this material (the detailed composition was confidential) is similar to AISI 630 with some additive elements therefore, it is considered as a modified- AISI 630. However, the composition (in wt. %) of the AISI 316 L SS is C 0.02; Mo 2.5; Cr 17; Ni 12; Fe balance. The AISI 316L SS was used for comparison purposes. Before each test, the exposed surface of SS samples was polished with 4000 SiC papers and washed with deionised water. The open circuit potential was stabilized within 60 min at room temperature. The cell was equipped so that the temperature during each experiment is kept constant.

Physical Characterization

The morphology of stainless steel surfaces after 60 min immersion in chloride solutions before and after adding SePA was checked by JEOL type 5600 scanning electron microscope.

The distribution of species in the adsorbed films was determined by depth profiling using Glow discharge optical emission spectroscopy (GDOES) type JobinYvon GD Profiler instrument operating at a pressure of 650 Pa and a power of 30 W in argon atmosphere. This low power is retained to decrease the speed of abrasion of the films with low thickness and to obtain maximum information at the surface. Quantified compositional results were evaluated automatically using the standard JobinYvon quantum intelligent quantification software.

Results and Discussion

Figure 2 shows the evolution of Rp for both SS specimen with SeAP concentration (C_{SeAP}/mg L^{-1}) and the rotation speed (Rot/rpm) of the working electrode. As it can be seen from the curves, optimum conditions relative to the highest Rp values for modified-AISI 630 and AISI 316L samples were $C_{SeAP} = 0.48 \pm 0.1$ mg L^{-1} and Rot = 3 ± 1 rpm. Based on this result, we kept these values constant in all experiences.

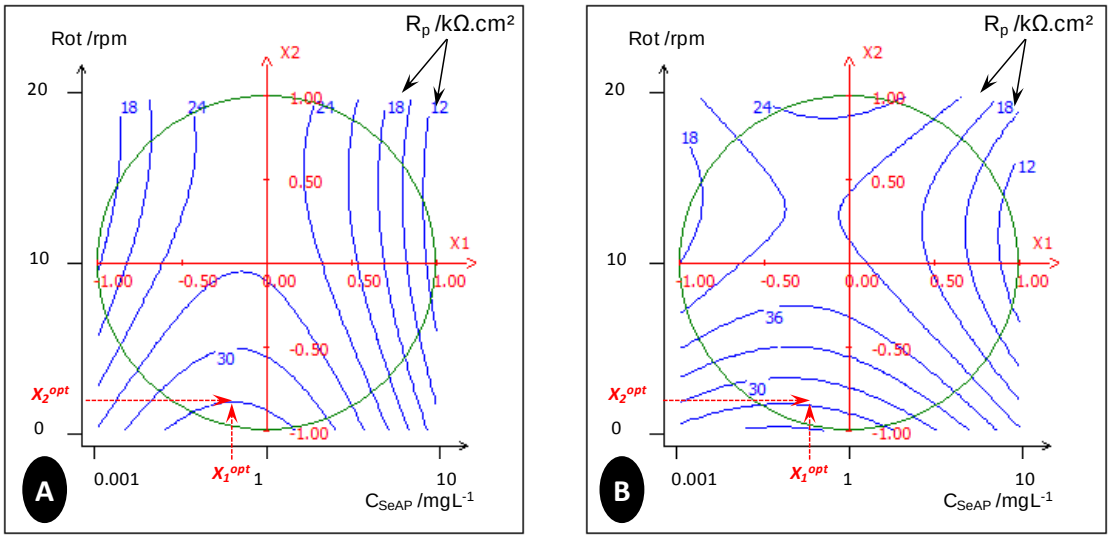

		X_i : Factors	
		X_1	X_2
Experimental field	Low limit (-)	0.001	10
	Upper limit (+)	5	20
Optima Conditions	X_i Optimum	0.48	3

Mathematical approach for the responses equation:

$$Y = 21.5 - 5.2\,X_1 - 3.6\,X_2 + 8.9\,X_{12} - 7.6\,X_{22} - 0.2\,X_1X_2$$

X_1: C_{SeAP} (mg.L^{-1}): SeAP content into the corrosive media.
X_2: Rot (rpm): electrode rotation speed.
Y : Rp (kΩ.cm²): polarization resistance of the sample.

Figure 2. Isoresponse curves for the modeling polarization resistance Rp (kΩ cm^2) of (A): modified-AISI630and(B):AISI 316L Stainless Steel substrates function of SeAP concentration (C_{SeAP}) and electrode rotation speed (Rot) into the corrosive media.

Potentiodynamic polarization

The potentiostatic polarization measurements for both AISI 630 and AISI 316L at a scan rate of 25mv/min are shown in Figure 3. These tests were conducted at a potential range varying from -1500 to 500 mV/SCE into 3 wt. % NaCl solution before and after adding different concentrations of SeAP. The inhibition efficiency for each concentration of inhibitor was calculated using the following equation [15]:

$$IE\% = \left(\frac{I_{corr} - I_{inh}}{I_{corr}}\right) \times 100$$

I_{corr} and I_{inh} are the corrosion current densities of the studied stainless steel without and with adding the inhibitor, respectively. The electrochemical parameters such as corrosion current density (I_{corr}), corrosion potential (E_{corr} vs. SCE), cathodic and anodic Tafel slopes (β_c, β_a) and inhibition efficiency (IE %) are gathered in Table 1.

As it can be seen in Figure 3, the increase of inhibitor concentrations decreases the corrosion current densities for both modified-AISI 630 and AISI 316L. For both types of SS, anodic current densities were decreased indicating that the SeAP inhibitor suppressed the anodic reactions. One should also note that the anodic peak observed on AISI 316L curve has disappeared after adding the inhibitor (Figure 3-B). This phenomenon can be due to the existence of N-P-N bonds having high electron density [16-17].

On the other hand, in the presence of the inhibitor, the both cathodic and anodic Tafel slopes of the modified-AISI 630 and AISI 316L almost remain unchanged, indicating that the inhibitor acted by merely blocking the reaction sites of the metal surface without changing the anodic and cathodic reaction mechanisms [18].

Table 1. Corrosion parameters derived from polarization measurements in chloride solution containing different concentrations of the SeAP inhibitor at room temperature

Sample	I_{corr} (mA.cm^{-2})	E_{corr} (mV vs. SCE)	$-\beta_c$ (mV dec^{-1})	β_a (mV dec^{-1})	%IE
Modified-AISI 630	1.820	-1040	62	24	-
Modified-AISI 630+ 0.1% SeAP	0.710	-890	134	85	45.1
Modified-AISI 630+ 0.3% SeAP	0.560	-840	152	82	69.2
Modified-AISI 630+ 0.5% SeAP	0.233	-810	162	80	78.2
AISI 316L	3.161	-189	155	90	-
AISI 316L + 0.1% SeAP	1.011	-40	126	87	68.1
AISI 316L + 0.3% SeAP	0.871	10	122	85	80.4
AISI 316L + 0.5% SeAP	0.422	51	118	82	91.7

The overall results reveal that the novel synthesized inhibitor acts with mixed-type inhibition[19]. It is observed that the inhibition efficiency increases with increasing concentration of the inhibitor and the highest inhibition efficiency reaches a maximum value of 78% for modified-AISI 630 and 91% for AISI 316L , both at 0.5 wt.% of SeAP (Table 1).

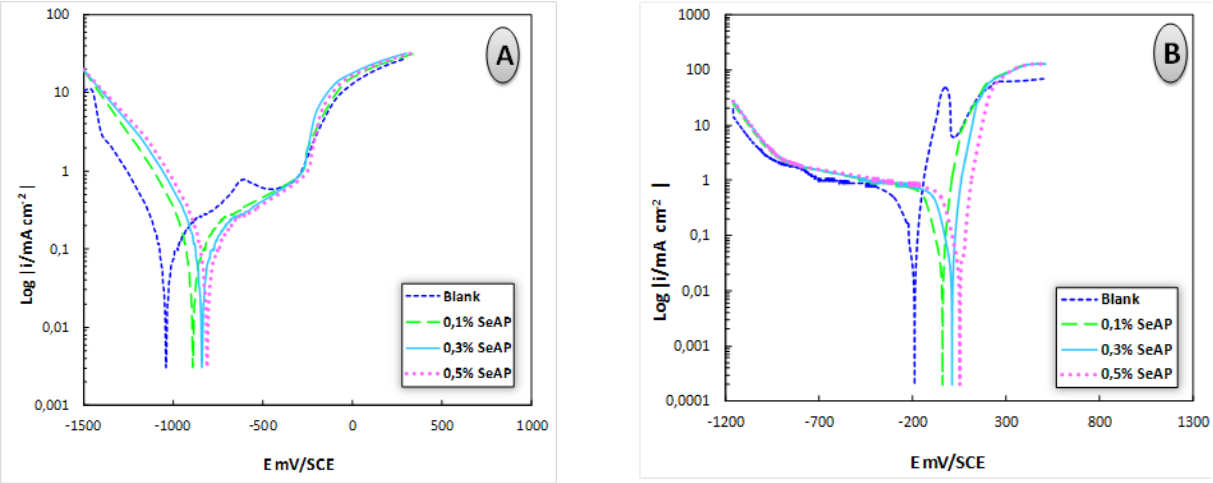

Figure 3. Polarization curves of (A): Modified- AISI 630 and (B): AISI 316L Stainless Steel in 3 wt. % NaCl containing different concentration of SeAP

Surface characterizations

SEM micrographs obtained for modified-AISI 630 and AISI 316L stainless steel surfaces after 60min immersion in sodium chloride solution at room temperature before and after adding SeAP at its optimum concentration, are shown in Figure 4.

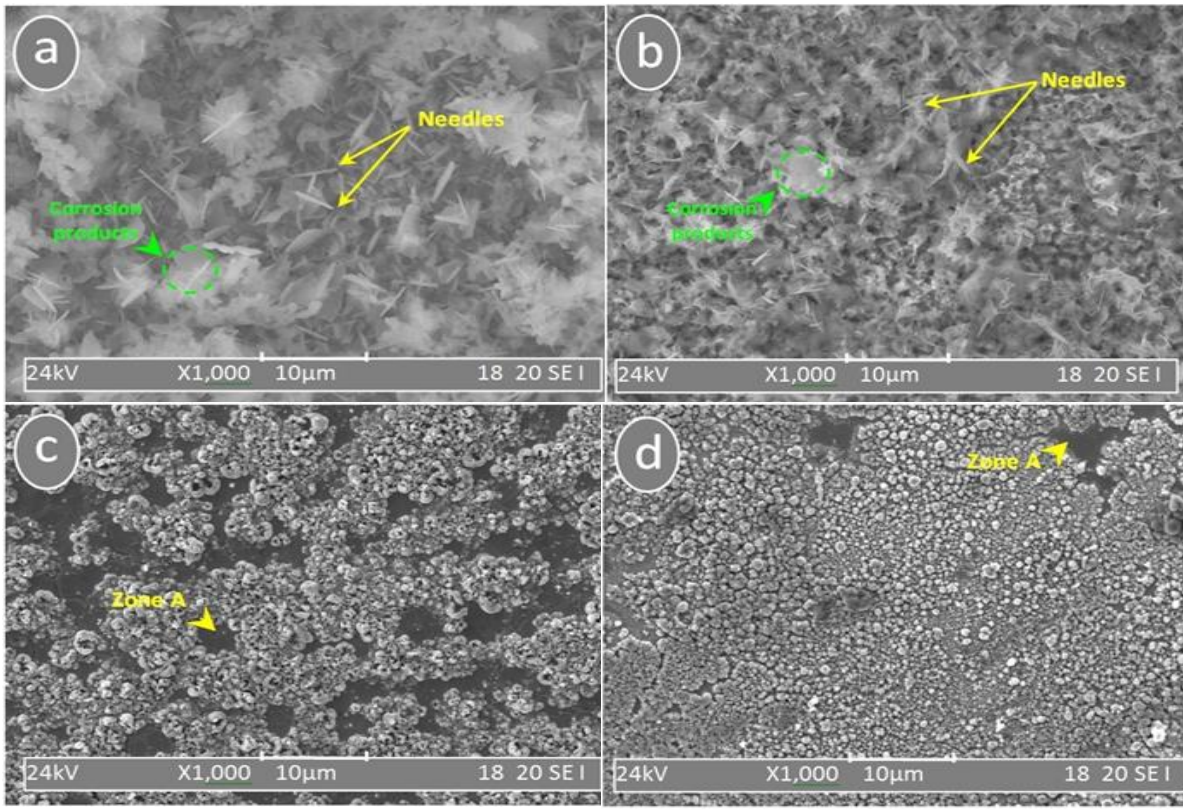

Figure 4. (a) SEM images of modified-AISI 630 and (b) AISI 316L SS both into 3 wt. % NaCl solution, (c) modified-AISI 630 and (d) AISI 316L SS both into 3 wt. % NaCl+0.5 wt. % SeAP solution

It can be seen from Figure 4-a and Figure 4-b that the alloy surfaces are strongly damaged without the inhibitor (uniform and corrosion products). One should also note the presence of well-defined needles on both modified-AISI 630 and AISI 316L surfaces that characterize chloride crystals [20-21]. At this zone, the Energy Dispersive Spectroscopy (EDS) spectrum demonstrates the presence of 70% of Chloride which has been referred to a massive diffusion of chloride ions into corrosion products.

When adding the SeAP, it can be seen that the rate of corrosion is decreased (Figure 4-c and d). In these SEM micrographs, zone A refers to the uncovered stainless steel surfaces. For both types of SS, Zone A indicates a stable metallic surface; neither cracks nor pits are visible. Moreover, it is found that after the addition of SeAP, an adsorbed layer inhibiting the corrosion is formed on both surfaces. EDS spectrum at this zone reveals the presence of 60% of carbon specific to the organic adsorbed inhibitor. However, Figure 4-c clearly shows that the addition of the SeAP leads to the formation of a stiffly stuck surface cover with irregular structures (probably due to the drying up of the hydrated compound). Such results have been reported elsewhere [20- 21].

Figure 5-A and B showed a comparison of GDOES depth profile of chloride incorporation and content into SeAP adsorbed film on modified-AISI 630 and AISI 316L surfaces, respectively. The contents of Na, C, N and H were removed from registered spectra to simplify the profile interpretation and to minimize the errors on the wt. %.

Indeed, the adsorbed film on AISI 316L surface is ~10µm thick. The SeAP adsorbed on modified-AISI 630 instead, is only ~ 2.5µm thick. This result is according to the SEM morphology observed in Figure 4-c and d. Hence, we can conclude that the proliferation of the organic compound on AISI 316L stainless steel is faster in both directions horizontally (totally covering the metallic surface) and vertically (enhancing the film thickness) when compared to its adsorption on modified-AISI 630 stainless steel. This behavior is related to the affinity of Nickel (contained in AISI 316L) to organic compounds especially phosphorus-containing inhibitors as mentioned elsewhere [22-23]. On the other hand, the wt. % content of phosphorus is twice higher in the adsorbed film on AISI 316L than in the one adsorbed on modified-AISI 630 (40 vs. 20 wt. %). Moreover, chloride incorporation into SeAP layer is represented in Figure 5-A where, the slow adsorption rate for SeAP in the case of modified-AISI 630 could be referred to its high surface activity as a martensitic stainless steel.

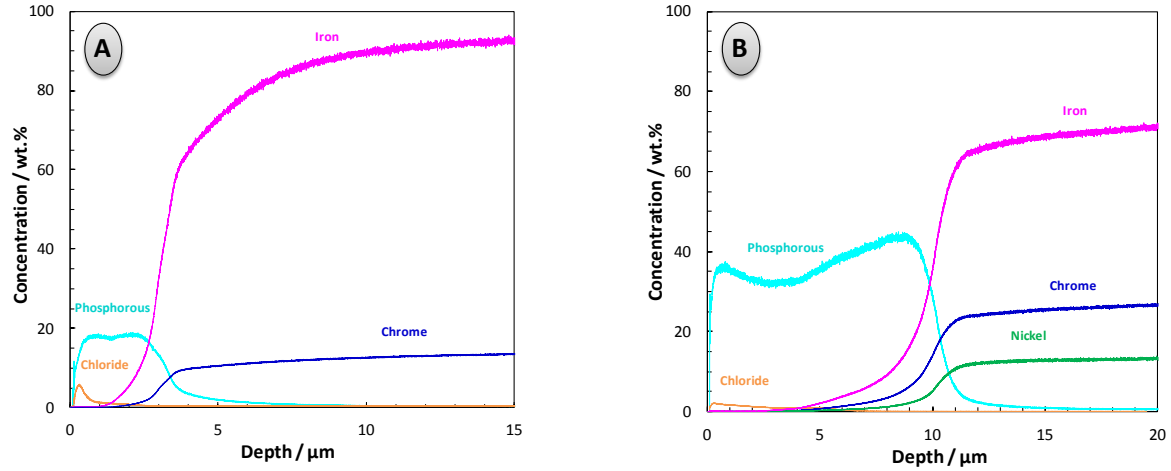

Figure 5. GDOES depth quantified profile of (A): modified-AISI 630 and (B): AISI 316L Stainless Steel in 3% NaCl containing 0.5% of SeAP

Conclusions

The influence of SeAP on modified-AISI 630 and AISI 316L SS corrosion in sodium chloride solution 3wt. %, has been investigated through potentiodynamic polarizations tests, GDOES and SEM.

The obtained results show that the inhibition efficiency improves at high concentration of SeAP in both types of stainless steel. The synthesized inhibitor acts as mixed-type (anodic and cathodic) in a merely neutral solution (pH=6.8). SEM and GDOES analysis clearly indicate the presence of a protective layer over the modified-AISI 630 and AISI 316L surfaces. Overall, the conclusions drawn from our results assert the efficiency of the SeAP compound as a novel inhibitor for stainless steel corrosion into chloride media.

Acknowledgments

We would like to acknowledge the material support provided by "La plateforme pétrolière de Oudhna au Nord de la Tunisie''.

References

1- Viswanathan S. Saji, Recent Patents on Corrosion Science, **2010**, 2, 6-12.
2- A. Yildirim, M. Cetin, Corros.Sci., **2008**, 50, 155-165.
3- M. Bartos, N. Hackerman,J. Electrochem. Soc., **1992**, 139**,** 3428-3433.
4- F. Kandemirli, S. Sagdinc, Corros. Sci., **2007**, 49, 2118-2130.
5- P. T. Tang, G.B. Nielsen, P.Moeller, Plat. Surf. Finish, **2009**, **81**, 20-23.
6- S. P. Kumaraguru, B. Veeraraghavan, B.N. Popov, J. Electrochem. Soc, **2006**, 153, 253-259.
7- W. Liang, X. Xiaolei, X. Jiujun, S. Yaqin, Thin Solid Films, **2001**, 391, 11-16.
8- M.K. Lei, X.M. Zhu, Surf. Coat. Technol, **2005**, 193, 22-28.
9- R. L. Liu, M.F. Yan, Surf. Coat. Technol., **2010**, 204, 2251-2256.
10- R. D. K. Misra, C. Y. Prasad, T.V. Balasubramanian and P. Rama Rao, sci., metal., **1987**, 21, 1067-1070.
11- R. D. K. Misra, C. Y. Prasad, T. V. Balasubramanian and P. Rama Rao, Sci., metal, **1986**, 20, 713-716
12- R.M. Davison, ASM Handbook, Corrosion, **1992**, 13-547.
13- S. A. Tavara, M.D. Chapetti, J.L. Otegui, C. Manfredi, InternationalJournal of Fatigue, **2001**, 23, 619-626.
14- W. E.Slinkard et Meek, Inorg.Chem., **1969**, 71, 1811.
15- W. Sassi, L. Dhouibi, P. Berçot, M. Rezrazi, E. Triki, Surf. Coat. Technol, **2012**, 206**,** 4235-4241.
16- T. X. Wu, Z. J. Li, J. C. Zhao,Chem. J. Chin. Univ., **1998,** 19, 1617-1625.
17- J. Wang, C. Cao, J. Chen, M. Zhang, G. Ye, H. Lin, J. Chin. Soc. Corros., Protect, **1995**, 15, 241-248.
18- S.M.A. Hosseini, A. Azimi, Corros. Sci,, **2009**, 51, 728-732.
19- M. Behpour, S.M. Ghoreishi, M. Salavati-Niasari, B. Ebrahimi, Chem. Phys,, **2008**, 107, 153-157.
20- W. Sassi, L. Dhouibi, P. Berçot, M. Rezrazi, Appl. Surf. Sci,, **2012**, 263**,** 373-381.
21- M. Rincón-Ortíz, M.A. Rodríguez, R.M. Carranza, R.B. Rebak, Corros. Sci,, **2013**, 68, 72-83.
22- R.V. Kashkovskiy, Y.I. Kuznetsov, L.P. Kazansky, Corros. Sci,, **2012**, 64, 126-136.
23- A. R. Grayeli-Korpi, H. Savaloni, App. Surf. Sci,, **2012**, 258, 9982- 9988.